Journal of Solid Mechanics Vol. 14, No. 1 (2022) pp. 89-98
DOI: 10.22034/jsm.2021.1899087.1591

Free Torsional Vibration Analysis of Hollow and Solid Non-Uniform Rotating Shafts Using Distributed and Lumped Modeling Technique

A. Saghafi *, M.A. Azizi

Department of Mechanical Engineering, Birjand University of Technology, Birjand, Iran

Received 1 November 2021; accepted 4 January 2022

ABSTRACT

In this paper, the torsional free vibration of solid and hollow rotating shafts with non-uniform tapered elements are investigated. To this end, the exact solution and also transfer matrix for the free torsional vibration of a hollow tapered shaft element with uniform thickness and also solid element are firstly obtained. Then, the natural frequencies are determined based on distributed and lumped modeling technique (DLMT). This technique is similar to transfer matrix method (TMM) but the exact solution is employed to obtain the transfer matrixes of the distributed element, therefore, there is no approximation and the natural frequencies and mode shapes are the exact values. To confirm the reliability of the presented method, the simulation results are compared with the results obtained from the other methods such as finite element method. It is shown that the proposed method provides highly accurate results and it can be simply applied to the complex torsional systems.

Keywords: Torsional vibration; Hollow tapered shaft; Distributed and lumped modeling techniques (DLMT); Transfer matrix method (TMM); Natural frequency.

1 INTRODUCTION

THE rotary systems are very important part of industrial machinery. These systems are mostly used in milling machines, machine tools, gear systems, axial pumps and turbines. All of these systems have a rotary shaft with an arbitrary number of concentrated elements, such as gear, disks, fans and spindles. Different harmonic and non-harmonic loads in the form of axial, transversal, and or torsional are imposed on its different components. Many researchers have investigated and analyzed torsional vibration of rotary systems. For example, Qing and Cheng [1] investigated the coupled torsional and flexural vibrations of rotor systems using finite element method (FEM). Koser and Pasin [2] proposed an analytical approach for analyzing torsional vibrations of shafts having variable inertia. Tabassian [3] analyzed the free torsional vibration of shafts by employing the adomian decomposition method (ADM). Boukhalfa et al. [4] analyzed free vibration of rotating composite shafts contains rigid disks using the p-Version of the finite element method. Chen et al. [5] studied the torsional vibration of a rotating shaft with multiple

*Corresponding author. Tel.: +98 915 5621075.
E-mail address: a.saghafi@birjandut.ac.ir (A.Saghafi)

disks and elastic support. Many studies have been done to investigate the torsional vibration of uniform shafts, however, dynamic of non-uniform cross section shafts are rarely investigated in the literature. For example, Chen [6] studied free torsional vibrations of a varying cross section cylinder with an adhesive mass. Wu [7] presented the exact solution for free torsional vibration of a linear conic shaft containing several concentrated elements. Typically, it is difficult or not possible to get the exact analytical solution for torsional free vibration of complex shafts containing several uniform and non-uniform elements along the shaft. The approximate methods such as finite element and transfer matrix method are capable for solving complex torsional system. For example, Nagaraj and Sahu [8] studied the torsional vibrations of non-uniform rotating blades by using FEM. Wu [9] presented a tapered shaft element and determine the torsional vibration characteristics of a damped rotating shaft system by using FEM.
The simplest approach which has been used extensively, is transfer matrix method (TMM). This method firstly proposed by Myklestad [10] and later extended by Prohl [11]. Wu and Yang [12] examined torsional and transversal vibration of rotary shafts by using TMM. Hsieh et al. [13] modified TMM for the coupled lateral and torsional vibrations of rotor-bearing systems. As is well known, the transfer matrix method [10- 14] and finite element method [8, 9] are two of the most popular methods for analyzing torsional vibration of non-uniform rotating systems. However, these methods are not accurate and so, the vibration characteristics obtained using these methods are approximate. On the other hand, the existing analytical methods [6, 7] are very accurate but they are limited to only to simple cases. Based on distributed lumped modeling technique, this paper presents an analytical formulation for free torsional vibration of hollow and solid non-uniform tapered shafts containing several concentrated elements. Distributed and lumped modeling technique (DLMT) is an efficient analytical method, which is based on the transfer matrix method. This method was described by Whalley for the second order systems [15]. The DLMT applied by Aleyaasin et al. [16] to analyze the flexural vibration of a rotating shaft. Recently, DLMT is implemented to modelling and compute the longitudinal, transversal and torsional vibration analysis. This technique is similar TMM but the exact solution is employed to obtain the transfer matrixes of the distributed element, therefore, there is no approximation and the natural frequencies and mode shapes are the exact values. DLMT can be easily applied to more complex systems, the results are very accurate and no approximation is used.

This paper is organized as follows. In section 2, the Distributed and lumped modeling technique is introduced. In section 3, the exact solution and also transfer matrix for the free torsional vibration of hollow and solid tapered shaft elements are calculated and used in DLMT. To verify the accuracy and reliability of proposed method, section 4 gives the comparison between the results obtained with proposed method and those obtained from the other methods.

2 THE DISTRIBUTED AND LUMPED MODELING TECHNIQUE

In this section, distributed and lumped modeling technique for torsional vibration of rotary shafts is introduced [17, 18]. A rotary shaft is considered as a combined set of distributed and lumped elements. Distributed elements are the shaft with various shapes, and the lumped elements are the components and parts which are mounted on the shaft, such as fans, disks and gears. The response of each element is an input for the next element as shown in Fig. 1.

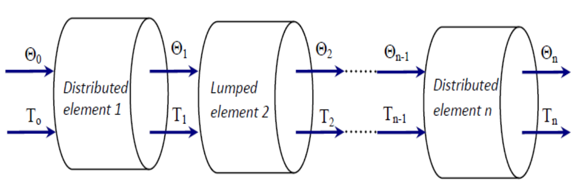

Fig.1
Distributed and lumped element.

For each element the transfer matrix are expressed in general form as:

$$\{Z\}_i = [H]_i \{Z\}_{i-1} \tag{1}$$

$\{Z\}_i$ and $\{Z\}_{i-1}$ are called state vectors in nodes i^{th} and i-1^{th}, respectively. Square matrix $[H]_i$ is transfer matrix for i^{th} element. Components of state vectors $\{Z\}$ are torsional angle θ, and torsional torque T. for the first element, the relationship between the state vector in node 1 and 0 can be expressed as:

$$\{Z\}_1 = [H]_1 \{Z\}_0$$

For the second and third elements:

$$\begin{aligned} \{Z\}_2 &= [H]_2 \{Z\}_1 = [H]_2 [H]_1 \{Z\}_0 \\ \{Z\}_3 &= [H]_3 \{Z\}_2 = [H]_3 [H]_2 [H]_1 \{Z\}_0 \end{aligned} \tag{2}$$

Finally, the relationship between the state vector in node n and state vector in node 0 can be expressed as:

$$\begin{aligned} \{Z\}_n &= [H]_n [H]_{n-1} \ldots [H]_2 [H]_1 \{Z\}_0 \\ \{Z\}_n &= [H]\{Z\}_0 \end{aligned} \tag{3}$$

where $[H]$ is total transfer matrix of the entire structure obtained from multiplication of all transfer matrices. This system is expressed as relation between boundary condition at two ends of system, node 0 and n. The vibration characteristics of system such as natural frequencies can be obtained by applying the boundary conditions. In the next section, transfer matrix for the free torsional vibration of hollow and solid distributed tapered elements is derived and then used in DLMT.

3 TRANSFER MATRIX FOR HOLLOW AND SOLID DISTRIBUTED TAPERED ELEMENTS

In this section the exact solution and also transfer matrix for free torsional vibration of hollow and solid distributed tapered shaft elements are derived. For free torsional vibration of non-uniform shaft, the dynamic equation can be expressed as [17]:

$$\frac{\partial}{\partial x}\left[GJ(x) \frac{\partial \tilde{\theta}(x,t)}{\partial x} \right] = I(x) \frac{\partial \tilde{\theta}^2(x,t)}{\partial t^2} \tag{4}$$

where, ρ is mass density, G is shear modulus, $I(x)$ and $J(x)$ are mass and area moment of inertia, respectively. (x, t) is the torsional angle of the shaft element at position x and time t. Fig. 2 shows a schematic of a hollow tapered shaft element. The tapered element has a length of L and the thickness of t. D_{Lo} and D_{Ro} are denote the outer diameters of the left and right side of the shaft, while the inner diameters of the left and right side of the shaft are D_{Li} and D_{Ri} , respectively. For this tapered element the diameter $D(x)$ at position x, can be obtained as:

$$D_o(x) = D_{Lo}(1 - \alpha \frac{x}{l}), \quad D_i(x) = D_{Li}(1 - \alpha \frac{x}{l}) \tag{5}$$

where:

$$\alpha = \frac{D_{Lo} - D_{Ro}}{D_{Lo}} \tag{6}$$

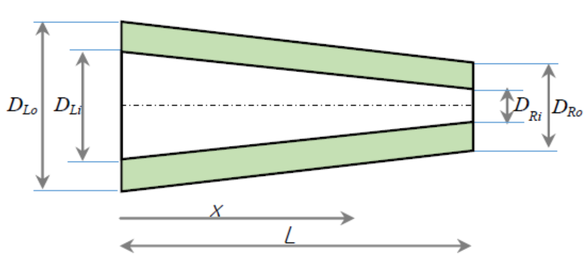

Fig.2
Schematic of a hollow tapered shaft element.

The area and mass moment of inertia for the considered element are varying with the coordinate x and are given as:

$$J(x)=\frac{1}{32}\pi(D_o(x)^4-D_i(x)^4)=\frac{\pi(D_{Lo}^4-D_{Li}^4)}{32}[1-\alpha(\frac{x}{l})]^4$$
$$I(x)=\frac{\rho\pi(D_{Lo}^4-D_{Li}^4)}{32}[1-\alpha(\frac{x}{l})]^4=\rho J(x) \tag{7}$$

where, $m(x)$ is the mass per unit length. To obtain the solution of Eq. (4), separation of variables is employed.

$$\tilde{\theta}(x,t)=\theta(x)q(t) \tag{8}$$

Assuming the harmonic motion one can conclude that:

$$\frac{\partial^2\tilde{\theta}}{\partial t^2}=-\omega^2\theta(x)q(t) \tag{9}$$

where, ω is natural frequency. Substituting Eq. (9) and Eq. (8) in Eq. (4) yields:

$$G(\frac{\pi(D_{Lo}^4-D_{Li}^4)}{32}[1-\alpha(\frac{x}{l})]^4)\frac{d^2\theta(x)}{dx^2}q(t)+4G\frac{\pi(D_{Lo}^4-D_{Li}^4)}{32}(1-\alpha\frac{x}{l})^3(-\frac{\alpha}{l})\frac{d\theta(x)}{dx}q(t)$$
$$=-\omega^2\rho(\frac{\pi(D_{Lo}^4-D_{Li}^4)}{32}[1-\alpha(\frac{x}{l})]^4)\theta(x)q(t) \tag{10}$$

By algebraic manipulation, the above equation is reduced to:

$$X\frac{d^2\theta(X)}{dX^2}+4\frac{d\theta(X)}{dX}+X\theta(X)=0 \tag{11}$$

where $\beta^2=\rho\omega^2/G$ and $X=\beta((l-\alpha x)/\alpha)$. This equation is Bessel differential equation. Its general solution is represented as:

$$\theta(X)=c_1X^{-\frac{3}{2}}J_{-\frac{3}{2}}(X)+c_2X^{-\frac{3}{2}}J_{\frac{3}{2}}(X) \tag{12}$$

so:

$$\theta(x)=(\beta(\frac{l}{\alpha}-x))^{-\frac{3}{2}}[c_1J_{-\frac{3}{2}}(\beta(\frac{l}{\alpha}-x))+c_2J_{\frac{3}{2}}(\beta(\frac{l}{\alpha}-x))] \tag{13}$$

The torsional torque can be obtained as:

$$T(x)=GJ(x)[\partial\theta(x)/\partial x]$$
$$=\frac{-G\beta\pi(D_{Lo}^4-D_{Li}^4)}{32}(1-\alpha\frac{x}{l})^4(\beta(\frac{l}{\alpha}-x))^{-\frac{3}{2}}[c_1J_{-\frac{5}{2}}(\beta(\frac{l}{\alpha}-x))-c_2J_{\frac{5}{2}}(\beta(\frac{l}{\alpha}-x))] \tag{14}$$

Eq. (13) and Eq. (14), can be written in the matrix form as:

$$\begin{Bmatrix} \theta(x) \\ T(x) \end{Bmatrix} = (\beta(\frac{l}{\alpha}-x))^{-\frac{3}{2}} \begin{bmatrix} J_{-\frac{3}{2}}(\beta(\frac{l}{\alpha}-x)) & J_{\frac{3}{2}}(\beta(\frac{l}{\alpha}-x)) \\ \frac{-G\beta\pi(D_{Lo}^4-D_{Li}^4)}{32}(1-\alpha\frac{x}{l})^4 J_{-\frac{5}{2}}(\beta(\frac{l}{\alpha}-x)) & \frac{G\beta\pi(D_{Lo}^4-D_{Li}^4)}{32}(1-\alpha\frac{x}{l})^4 J_{\frac{5}{2}}(\beta(\frac{l}{\alpha}-x)) \end{bmatrix} \begin{Bmatrix} c_1 \\ c_2 \end{Bmatrix} \tag{15}$$

or in the compact form:

$$\{Z(x)\} = \left[\tilde{H}(x)_{htd}\right].\{C\} \tag{16}$$

where $\{Z\}$ and $\{C\}$ are state and coefficient vectors, respectively. Using the boundary conditions at nodes i-1, where x = 0, $\{Z(0)\}$= $\{Z_{i\text{-}1}\}$, Eq. (16) can be expressed as:

$$\{Z_{i-1}\} = \left[\tilde{H}(0)_{htd}\right].\{C\} \tag{17}$$

The coefficient vector $\{C\}$ can be obtained as:

$$\{C\} = \left[\tilde{H}(0)_{htd}\right]^{-1}.\{Z_{i-1}\} \tag{18}$$

Then, substituting $\{C\}$ in Eq. (16), the following matrix equation is obtained:

$$\{Z(x)\} = \left[\tilde{H}(x)_{htd}\right].\left[\tilde{H}(0)_{htd}\right]^{-1}.\{Z_{i-1}\} \tag{19}$$

At node i, where x = l, state vector will be $\{Z(l)\}$= $\{Z_i\}$. Therefore, the relationship between the state vector in node i and node i-1, can be expressed as:

$$\{Z_i\} = \left[\tilde{H}(l)_{htd}\right].\left[\tilde{H}(0)_{htd}\right]^{-1}.\{Z_{i-1}\} = \left[H_{htd}\right]_i.\{Z_{i-1}\} \tag{20}$$

where, the square matrix $[H_{htd}]_i$, is transfer matrix for hollow tapered distributed element in DLMT. Substituting (D_{Li}=0) in Eq. (20), the transfer matrix for a solid tapered element ($[H_{std}]_i$) can be obtained. For a uniform distributed element, and also lumped element the transfer matrix can be expressed as: [17, 18, 19]

$$\left[H_{ud}\right]_i = \left[\tilde{H}(l)_{ud}\right].\left[\tilde{H}(0)_{ud}\right]^{-1} = \begin{bmatrix} \cos(\beta \mathrm{L}) & \sin(\beta \mathrm{L})/\mathrm{GJ}\beta \\ -\mathrm{GJ}\beta\sin(\beta \mathrm{L}) & \cos(\beta \mathrm{L}) \end{bmatrix} \tag{21}$$

$$\left[H_l\right]_i = \left[H_P\right]_i.\left[H_f\right]_i = \begin{bmatrix} 1 & 0 \\ -(\omega^2 J - i\,\omega c_0) - \bar{m} & 1 \end{bmatrix} . \begin{bmatrix} 1 & \frac{1}{K_i + i\,\omega c_i} \\ 0 & 1 \end{bmatrix} = \begin{bmatrix} 1 & \frac{1}{K_i + i\,\omega c_i} \\ -(\omega^2 J - i\,\omega c_0) - \bar{m} & 1 - \frac{(\omega^2 J - i\,\omega c_0) + \bar{m}}{K_i + i\,\omega c_i} \end{bmatrix} \tag{22}$$

where, c_0 and c_i are damping coefficient of discs and shafts, respectively. $\bar{m}$ represent an excitation torque of the i^{th} element. $[H_{ud}]_i$ and $[H_l]_i$ are transfer matrixes for uniform distributed and lumped element, respectively.

4 NUMERICAL RESULTS AND DISCUSSIONS

In this section, in order to confirm the capability and accuracy of the presented method in torsional vibration analysis of shafts with non-uniform tapered elements, some examples are presented. The simulation results are compared with those obtained from the FEM and analytical method.

Case 1: Cantilever hollow tapered shaft (Clamped– Free)

As first case, a clamp hollow tapered shaft which right ends of the shaft is free (see Fig. 3) is studied. The geometry and material properties of the shaft are given in Table 1. This shaft is modeled by only one distribute hollow tapered element. The boundary condition can be expressed as:

$$\begin{Bmatrix}\theta \\ T\end{Bmatrix}_{x=0}=\begin{Bmatrix}0 \\ T(0)\end{Bmatrix}, \qquad \begin{Bmatrix}\theta \\ T\end{Bmatrix}_{x=L}=\begin{Bmatrix}\theta(l) \\ 0\end{Bmatrix}$$

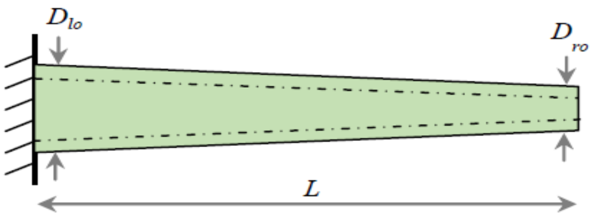

Fig.3
A cantilever hollow tapered shaft.

Table 1
Physical properties of the shaft.

shear modulus	$G=8.01\times10^{10}N/m^2$
density	$\rho=7820kg/m$
total shaft length	$l=1.8m$
outer diameter of left end	D_{lo}=0.045 *m*
outer diameter of right end	D_{ro}=0.03686 *m*
thickness of element	*t*=0.01 *m*

Using Eq. (20), the relationship between the state vector in node 1 and state vector in node 0, can be obtained. Frequency equation can be achieved by applying the boundary condition.

$$\{Z_1\}=[H_{htd}]_1\cdot\{Z_0\}=\begin{bmatrix}a_{11} & a_{12}\\ a_{21} & a_{22}\end{bmatrix}\{Z_0\}\Rightarrow\begin{Bmatrix}\theta(l)\\ 0\end{Bmatrix}=\begin{bmatrix}a_{11} & a_{12}\\ a_{21} & a_{22}\end{bmatrix}\begin{Bmatrix}0\\ T(0)\end{Bmatrix} \tag{23}$$

The natural frequencies could be obtained by solving Eq. (23). The first five natural frequencies are listed in Table 2. Based on FEM, the first five natural frequencies of the shaft are obtained by using 5, 50, 100 and 200 elements. The comparison results of the frequencies are summarized in Table 2. One sees that the natural frequencies obtained from DLMT are very close to the results obtained using the FEM, and confirm the accuracy of the presented method. Also, the results show that the difference of the frequency between FEM and DLMT is decreased with increase the number of element. The dimension of mass and stiffness matrixes in the FEM are $(n+1)\times(n+1)$, n is number of elements, while in the present modeling the final matrix is 2×2. As a consequence, the computational required by the proposed methods can be reduced significantly as compared with FEM. On the other hand, the DLMT is efficient and accurate.

Table 2
Comparison of the first five natural frequencies of the cantilever hollow tapered shaft.

mode	DLMT	FEM		Difference (%)
		Number of elements	Frequency (*rad/s*)	
1	3260.28	5	3278.60	0.005619149
		50	3260.45	5.21428E-05
		100	3260.32	1.22689E-05
		200	3260.28	0

2	8556.77	5	8890.51	0.039003035
		50	8560.06	0.000384491
		100	8557.59	9.58306E-05
		200	8556.96	2.22046E-05
3	14072.86	5	15545.01	0.104609155
		50	14087.55	0.001043853
		100	14076.53	0.000260786
		200	14073.77	6.46635E-05
4	19628.09	5	23227.76	0.183393799
		50	19667.98	0.002032291
		100	19638.06	0.000507946
		200	19630.58	0.000126859
5	25196.82	5	29844.25	0.184445101
		50	25281.22	0.003349629
		100	25217.89	0.000836217
		200	25202.08	0.000208757

Case 2: Free tapered shaft (Free– Free)

Fig. 4 shows a freely supported solid tapered shaft. The left and right diameter of the shaft are D_l =0.041 m and D_r=0.05125 m. The other material properties and geometries are similar to the case 1. This shaft is modeled by only one distribute solid tapered element, so transfer matrix can be expressed as: $[H_{std}]_1$. Frequency equation can be obtained by applying the boundary condition.

$$\{Z_1\}=[H_{std}]_1.\{Z_0\}=\begin{bmatrix} a_{11} & a_{12} \\ a_{21} & a_{22} \end{bmatrix}\{Z_0\}\Rightarrow\begin{Bmatrix} \theta(l) \\ 0 \end{Bmatrix}=\begin{bmatrix} a_{11} & a_{12} \\ a_{21} & a_{22} \end{bmatrix}\begin{Bmatrix} \theta(l) \\ 0 \end{Bmatrix} \tag{24}$$

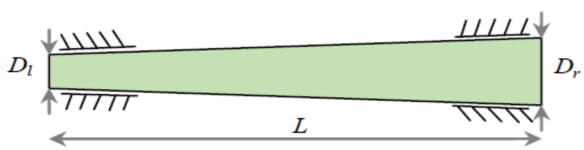

Fig.4
Freely supported tapered shaft.

The first five natural frequencies are listed in Table 3, and compared with the results obtained from other methods. It is seen that the results obtained from the proposed method are very close to the results reported by Ref. [9], and confirm the accuracy of the DLMT. To further investigation, mode shapes are also obtained. The first four mode shapes obtained from the presented method and FEM are shown and compared in Fig. 5. The accuracy of the results shows that the DLMT can be potentially used for the analysis of torsional systems.

Table 3
The first five natural frequencies of the freely supported tapered shaft.

	ω_1	ω_2	ω_3	ω_4	ω_5
DLMT	5669.49	11214.02	16785.84	22364.66	27946.28
Reference [9]	5670.15	11219.16	16803.15	22405.64	28026.28
FEM	5669.51	11214.21	16786.53	22366.29	27949.48

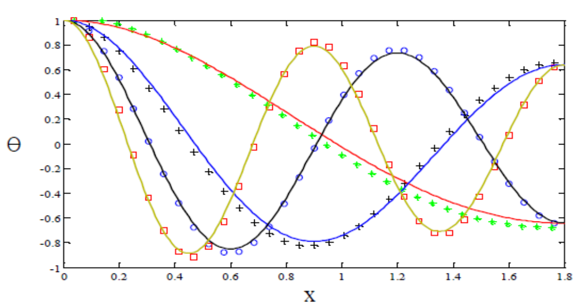

Fig.5
The first four normalized mode shapes of freely supported shaft. 1st (——), 2nd (——), 3td (——) and 4th (——) mode shape obtained from the DLMT and 1st (*), 2nd (+), 3td (∘) and 4th (□) mode shape obtained from the FEM.

Case 3: Cantilever tapered shaft with a lumped mass at the end

The third tapered shaft model is depicted in Fig. 6, which a disk is attached at one end. The mass moment of inertia is J=3.904×10^{-3} *kgm*^{2}. The other material properties and geometries are similar to the first case. The tapered shaft is regarded as a distributed element and the end mass as a lumped element, so transfer matrix can be expressed as: $[p]_2 . [H_{std}]_1$. Frequency equation can be obtained by applying the boundary condition.

$$\{Z_2\} = [p]_2 [H_{std}]_1 . \{Z_0\} = \begin{bmatrix} a_{11} & a_{12} \\ a_{21} & a_{22} \end{bmatrix} \{Z_0\} \Rightarrow \begin{Bmatrix} \theta(l) \\ 0 \end{Bmatrix} = \begin{bmatrix} a_{11} & a_{12} \\ a_{21} & a_{22} \end{bmatrix} \begin{Bmatrix} 0 \\ T(0) \end{Bmatrix} \tag{25}$$

The first five natural frequencies are listed in Table 4. It is seen that the natural frequencies obtained from the presented method are in good agreement with results reported by Ref. [9].

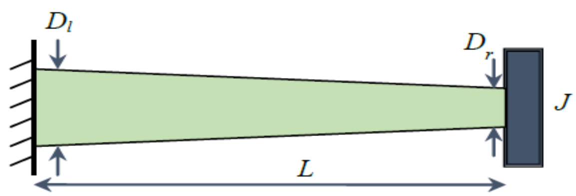

Fig.6
Cantilever tapered shaft with end mass.

Table 4
The first five natural frequencies of the cantilever tapered shaft with end mass.

	ω_1	ω_2	ω_3	ω_4	ω_5
DLMT	1573.36	5956.81	11365.03	16887.52	22441.19
Reference [9]	1573.39	5957.49	11370.22	16904.89	22482.24
FEM	1573.35	5956.84	11365.42	16888.21	22442.82

Case 4: Free tapered shaft with a lumped mass at the middle of length

Fig. 7 shows a freely supported solid tapered shaft carrying a rigid disk at the middle of length. The left and right diameter of the shaft are D_l =0.041 *m* and D_r=0.04497 *m*. The total shaft length and mass moment of inertia of the disk are L=2.4 *m* and J=4.583×10^{-3} *kg.m*^{2}, respectively. The other material properties and geometries are similar to the first case. Transfer matrix for this case can be expressed as: $[H_{std}]_3 . [p]_2 . [H_{std}]_1$. The first five natural frequencies calculated for this case are presented in Table 5, and compared with those reported by Wu [9]. It is obvious that the results calculated by the two methods are in good agreement.

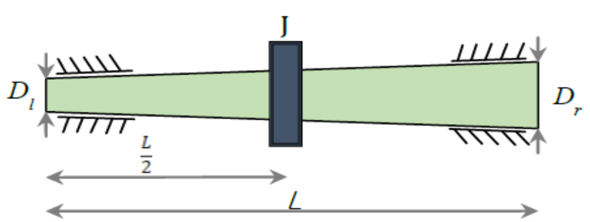

Fig.7
Freely supported tapered shaft with a mass at the middle of length.

Table 5
The first five natural frequencies of the free tapered shaft with a lumped mass at the middle of length.

	ω_1	ω_2	ω_3	ω_4	ω_5
DLMT	4191.43	5719.46	12569.20	13289.82	20947.59
Reference [9]	4189.94	5698.64	12581.13	13289.91	21006.86
FEM	4189.72	5720.57	12568.58	13291.89	20948.39

Case 5: Transfer shaft of a generator

In order to show efficiency and the engineering application of proposed method, two generator transfer shafts are investigated. Fig.8 shows the schematic diagram of these transfer shafts. The material properties and geometries are given in Table 6. The transfer matrix of these shafts are obtained by DLMT. Also, the generator shafts are simulated in ANSYS. The first five natural frequencies are listed in Table 7, and compared with those obtained from DLMT. A very good agreement is shown between these results. The successful implementation of the DLMT for these cases further confirms the capability of the proposed method in vibration analysis of complex systems.

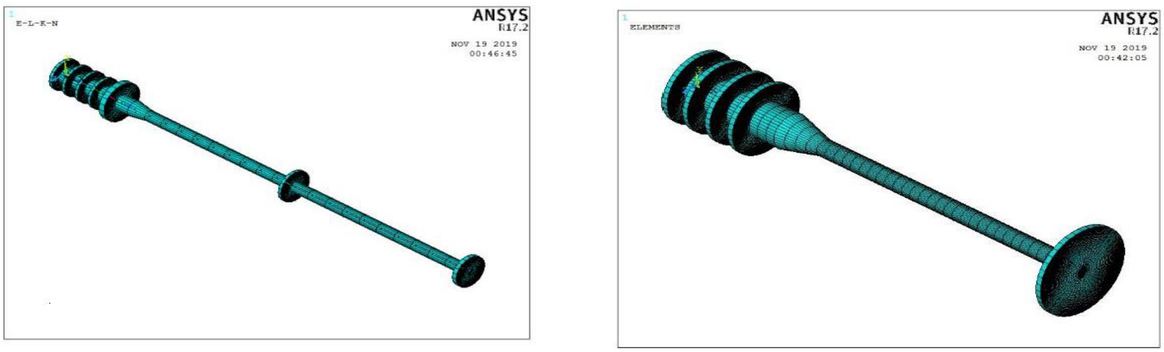

(a) (b)

Fig.8
The schematic diagram of generator transfer shafts.

Table 6
Physical properties of the transfer shafts.

shear modulus	$G = 8.01\times10^{10}\, N/m^2$
density	$\rho_s = 7820\, kg/m^3$
mass moment of inertia for disk 1,2,3,4	$J_1 = J_2 = J_3 = J_4 = 0.0308 kgm^2$
mass moment of inertia for disk 5	$J_5 = 1.4322 kgm^2$
mass moment of inertia for disk 6	$J_6 = 0.0279 kgm^2$
mass moment of inertia for disk 7	$J_7 = 0.4894 kgm^2$

Table 7
The first five natural frequencies of two transfer shafts.

	Transfer shaft (a)			Transfer shaft (b)	
	DLMT	Ref [9]	FEM	DLMT	FEM
ω_1	510.45	510.41	510.14	783.97	784.07
ω_2	2845.35	2845.85	2845.46	8465.39	8466.64
ω_3	6208.84	6211.09	6204.45	16054.64	16058.56
ω_4	7596.52	7617.05	7600.14	17697.11	17706.64
ω_5	9287.71	9320.98	9295.97	25296.88	25308.77

5 CONCLUSION

In this paper, the distributed lumped modeling technique has been employed to present an efficient analytical method and exact solution for analyses of the free torsional vibration of shaft with uniform and non-uniform tapered elements. Numerical example has been done and shows the reliability and accuracy of the proposed method. The proposed method is efficient and accurate technique and therefore it is recommended for vibration analysis of complex torsional systems.

REFERENCES

[1] Qing H.Q., Cheng X.M., 1996, Coupled torsional-flexural vibration of shaft systems in mechanical engineering- I, Finite element model, *Computers & Structures* **58**: 835-843.

[2] Koser K., Pasin F., 1997, Torsional vibrations of the drive shafts of mechanisms, *Journal of Sound and Vibration* **199**: 559-565.

[3] Tabassian R., 2013, Torsional vibration analysis of shafts based on Adomian decomposition method, *Applied and Computational Mechanics* **7**: 205-222.

[4] Boukhalfa A., Hadjoui A., Hamza C.S.M., 2010, Free vibration analysis of an embarked rotating composite shaft using the hp- version of the FEM, *Latin American Journal of Solids and Structures* **7**(2): 105-141.

[5] Chen M., Li Sh., Li H., Peng T., Liu S., 2018, New analytic method for free torsional vibration analysis of a shaft with multiple disks and elastic supports, *Archive of Applied Mechanics* **88**(6): 955-979.

[6] Chen Y.Z., 2001, Torsional free vibration of a cylinder with varying cross-section and adhesive masses, *Journal of Sound and Vibration* **241**(3): 503-512.

[7] Wu J.J., 2013, Torsional vibrations of a conic shaft with opposite tapers carrying arbitrary concentrated elements, *Marine Engineering and Applications* **2013**: 491062.

[8] Nagaraj V.T., Sahu N., 1982, Torsional vibrations of non-uniform rotating blades with attachment flexibility, *Journal of Sound and Vibration* **80**: 401-411.

[9] Wu J.J., 2007, Torsional vibration analyses of a damped shafting system using tapered shaft element, *Journal of Sound and Vibration* **306**(3-5): 946-954.

[10] Myklestad N.O., 1944, A new method of calculating natural modes of uncoupled bending vibration of airplane wings and other type of beams, *Journal of Aerospace Science* **11**: 153-162.

[11] Prohl M.A., 1945, A general method for calculating critical speeds of fiexible rotors, *Journal of Applied Mechanics* **12**: 142-148.

[12] Wu J.S., Yang I.H., 1995, Computer method for torsion-and-flexure-coupled forced vibration of shafting system with damping, *Journal of Sound and Vibration* **180**(3): 417-435.

[13] Hsieh S.C., Chen J.H., Lee A.C., 2008, A modified transfer matrix method for the coupled lateral and torsional vibrations of asymmetric rotor-bearing systems, *Journal of Sound and Vibration* **312**: 563-571.

[14] Bashir Asdaque P.M.G., Behera R.K., 2014, Vibration analysis of hollow tapered shaft rotor, *Advances in Acoustics and Vibration* **2014**: 410851.

[15] Whalley R., 1988, The response of distributed-lumped parameter systems, *Proceedings of the Institution of Mechanical Engineers* **202**(C6): 421-428.

[16] Aleyaasin M., Ebrahimi M., Whalley R., 2001, Flexural vibration of rotating shafts by frequency domain hybrid modelling, *Journal of Computers and Structures* **79**: 319-331.

[17] Meirovitch L., 1967, *Analytical Methods in Vibrations*, Macmillan, Company, London.

[18] Thomson W.T., 1988, *Theory of Vibration with Application*, Prentice-Hall.

[19] Yang M., Hu Y., Zhang J., Ding G., Song Ch., 2018, Study on forced torsional vibration of CFRP drive-line system with internal damping, *Applied Composite Materials* **25**(6): 1307-1322.